Design Process for a Scale Horizontal Axis Tidal Turbine Blade.

Robert Ellis [†*], Matthew Allmark [†‡], Tim O'Doherty [†§], Allan Mason-Jones [†¶], Stephanie Ordonez-Sanchez [‖ **], Kate Johannesen [‖ ††], Cameron Johnstone [‖ ‡‡]

[†]School of Engineering, Cardiff University
Cardiff, CF24 3AA United Kingdom
[*]EllisR10@cardiff.ac.uk
[‡]AllmarkMJ1@cardiff.ac.uk
[§]Odoherty@cardiff.ac.uk
[¶]Mason-JonesA@cardiff.ac.uk
[‖]Energy Systems Research Unit, University of Strathclyde
Glasgow, G1 1XJ, United Kingdom
[**]s.ordonez@strath.ac.uk
[††]kate.porter@strath.ac.uk
[‡‡]cameron.johnstone@strath.ac.uk

***Index Terms*—Computational Fluid Dynamics, ANSYS CFX, Marine Energy, Tidal Stream Turbines, Tidal Energy**

***Abstract*—If tidal energy extraction is to be maximised then emphasis needs to be placed on the design of the rotor geometry to optimise performance. The work documented in this paper describes the process used in the design and validation of a new blade based on the Wortmann FX63-137 aerofoil.**

BEMT was used as an initial tool to redesign the blade due to speed in which calculations can be completed. CFD models were produced after to incorporate the hydrodynamics and provide a 3D solution. The performance coefficients for C_P and C_T were calculated by each of the two computational methods for comparison with the experimental testing. The experimental testing was conducted at the INSEAN tow tank to provide validation for the computational models.

The CFD model was found to closely predict the performance coefficients of the turbine at low TSR at and peak power. The BEMT model over predicted both the C_P and the C_T when compared to the experimental work, however was found to be good as an initial method for redesigning the blade.

I. Introduction

The need to produce sustainable and commercially viable energy from renewable sources is becoming ever more apparent. All countries in the world except the USA have now signed up to the Paris Agreement [**?**] with the aim of keeping the global temperature rise below 2 degrees. The UK, being one of these countries, aims to have $15\,\%$ of all energy produced being supplied by renewable sources by 2020, up from $4.1\,\%$ in 2012 [1]. Findings by [2] concluded that wave and tidal stream could provide in the region of $20\,\%$ of the UK's electricity consumption if fully exploited with the areas of large interest including the Bristol Channel, Anglesey and the Pentland Firth. The latter of these locations is currently the focus of the MeyGen Project which has completed Phase 1A, the deployment and installation of four $1.5\,\mathrm{MW}$ turbines, and has now moved onto Phase 1B which involves the installation on another four $1.5\,\mathrm{MW}$ turbines [3]. With such potential from around UK coastline the need to develop durable and efficient turbines means that emphasis must be placed on the design of the turbine and blades to help realise the full energy potential.

To try and fully utilise the potential of the available resource then turbines must be designed to maximise power extraction. One key way of ensuring this is by placing the focus on the design of the blade to ensure that the C_P is optimised. Alongside this the loading that the turbine is subject to must be minimised to ensure the reliability and survivability of the devices placed in the water. Excessive loading on the turbine can lead to extra associated costs due to higher level of required maintenance. A balance between the two performance coefficients needs to be found to ensure the cost of the device, throughout its life, makes tidal energy commercially viable and long lasting.

CMERG, Cardiff University, has been using the Wortmann $FX63-137$ aerofoil, seen in Fig. 1, for its blade design since the first device was designed by [4]. The properties for this design can be found in Table I. The Wortmann profile was used as it has low stall and high lift characteristics [5]. It was designed with a large chord length and a high twist at the root of the blade to provide a self-starting capability. Development of a new turbine has led to the redesign of the blade whilst maintaining the Wortmann aerofoil.

The new turbine was to have a diameter of $900\,\mathrm{mm}$ compared to the previous turbine which was $500\,\mathrm{mm}$. The hub was to be $130\,\mathrm{mm}$ to allow for the instrumentation to be placed in the nose cone. Allowing for a $0.5\,\mathrm{mm}$ gap between the hub and the base of the blade, the total length of the blade, from root to tip, was increased to $384.5\,\mathrm{mm}$, from $190\,\mathrm{mm}$.

Other than the increase in the total blade length, three key areas were looked at for the new design; the blade twist from root to tip and the chord length. In addition to these design requirements a restriction was placed on the design; the C_P was to be greater than the original design and the C_T was to be not significantly increased. It was decided that the process would be done using the Blade Element Momentum Theory (BEMT), CFD and experimental work.

There has been a selection of previous work that has looked at comparisons between CFD, BEMT and experimental results using a variety of different models. Lee et al. [6] found a good comparison between their in house BEMT code and ANSYS Fluent for performance characteristics around the peak TSR, however there was a larger discrepancy for low and high TSR values. A comparison by Johnson et al. [7] looked at BEMT and ANSYS CFX using the SST $k-\omega$ turbulence model. For a range of TSR values between 2 - 3.6 BEMT was shown to under predict all performance coefficients at the lower end of the range. Masters et al. [8] found good agreement between

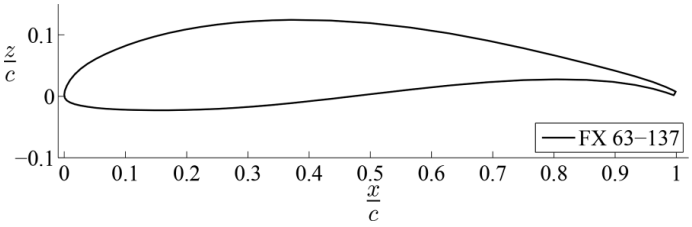

Fig. 1: *Wortmann FX63-137 aerofoil*

BEMT and experimental models and O'Doherty et al. [9] found good comparisons could be drawn between experimental results and ANSYS Fluent.

This paper aims to give a description of the design processes undertaken for the development of the new blade and provide comparisons of the performance characteristics between BEMT, CFD and experimental data.

TABLE I: Old Blade characteristics from Mason-Jones [10].

r/R	**Twist** (deg)	**Chord Length** (mm)
0.229	33.89	75.0
0.305	26.01	75.5
0.382	19.86	74.5
0.459	15.29	70.0
0.536	11.6	63.5
0.615	8.41	56.0
0.692	5.52	45.25
0.768	3.19	39.04
0.845	1.25	35.0
0.922	0.25	31.65
1.00	0.0	29.5

II. Methodology

A. Lift and Drag Coefficients

For the BEMT code, described fully in Section II-B, lift and drag coefficients that correspond to the relevant aerofoil are used. For the purpose of this work, when calcualting the lift and drag coefficnets for the aerofil, two main options were looked at; two-dimensional CFD models or the two-dimensional panel code XFoil [11].

Molland et al. [12] found that for a selection of NACA aerofoils XFoil gave good predictions for the C_L when compared to experimental work, however for angles above 7 degrees the values for C_D were found to be lower. Other work by Jo and Lee [13] found that CFD gave good predictions of lift and drag when compared to experimental results although Morgado et al. [14] found that XFoil gave a better prediction for both lift and drag when compared to the CFD based SST $k-\omega$ turbulence models. From this it was decided that XFoil was to be used when calculating the C_L and C_D values for use in the BEMT code.

B. Blade Element Momentum Theory

BEMT has been used extensively to calculate the performance characteristics of tidal stream turbines due to the comparative simplicity in which the code can be written and executed. Coupled with the small amount of time required to reach a solution it is an ideal method for comparing multiple rotor geometries. Limitations in BEMT do exist and correction factors need to be added to ensure the rotor is treated with a finite number of blades, rather than as a disk, and that tip and hub losses for the blades are accounted for [15].

Within momentum theory the turbine is modelled using a simple ideal permeable disk, or actuator disk, that is placed in a stream tube which is independent of the surrounding flow [16]. Equations can be derived for the two unknown induction factors based on the conservation of momentum. Details about the rotor geometry and the number of blades in the turbine are not included so the momentum theory is coupled with the blade element theory.

The blade element theory looks at resolving the forces on the blade, via an iterative approach, by breaking it into a number of independent radial elements. If the lift and drag coefficients are known for the aerofoil in question then the distribution of the forces along the blade can be found with respect to the induction factors [17]. The combination of the two sets of equations from the momentum and the blade element theories allows the performance of the turbine to be found.

The code used for the work conducted here was developed at Strathclyde University [18].

A selection of blade chord length distributions were considered. This was done to try and maximise the power coefficient whilst trying to keep the thrust coefficient to within $10\,\%$ of the original Wortmann FX63-137 blade used by Cardiff University [4]. Three examples of the final selection of chord lengths are shown in Table II. Blade one was now considered as the base case in the comparison. Blade two had a reduced chord length at the root of the blade and an increased chord length at the tip when compared to blade one. Blade three had the same chord length at the root of the blade when compared with blade one, but the chord length at the tip of the blade was similar to that of blade two.

TABLE II: Blade characteristics comparison

r/R	**Blade 1 Chord** (mm)	**Blade 2 Chord** (mm)	**Blade 3 Chord** (mm)
0.146	72.5	72.5	72.5
0.229	87.8	82.8	87.8
0.305	103.1	97.6	103.1
0.382	109.6	106.8	109.6
0.459	109.5	106.2	109.5
0.536	105.1	105.1	105.1
0.615	93.1	93.1	93.1
0.692	83.6	83.6	83.6
0.768	73.6	74.3	74.3
0.845	67.6	68.3	68.3
0.922	62.8	64.1	64.1
1.00	58.9	60.2	60.2

The areas of interest included looking at how changes to the root and tip chord length affected the performance characteristics. For each of the three blade designs a large selection of twist distributions from tip to root were looked at, ranging from 15-25 degrees. The pitch angle for the old blade was 6 degrees and so to determine the optimised set up for the blade a range of pitch angles between 5 - 8 degrees were looked at. In total there were 44 possible variations per blade so as to provide a wide comparison in the hope of optimising the blade design.

C. Computational Fluid Dynamics

Once the geometric characteristics had been finalised via BEMT a three-dimensional drawing was produced using SolidWorks for use in the commercial CFD code ANSYS CFX.

Design Modeller, the inbuilt CAD software in ANSYS workbench, was used to create the domain for the simulation. The turbine was

imported into the design space once drawn in SolidWorks. Two domains were created using the origin of the turbine as the reference point; the outer control volume and the moving reference frame (MRF). A boolean allowed the two domains to be separated from each other. In doing this the MRF could be treated as a separate body and therefore be allowed to rotate, simulating the rotation of the turbine. The turbine was subtracted from the MRF as CFX only solves for fluid components and treats all volumes in the domain as fluid, leaving a void with the outline of the turbine which would be used to create the interaction of the fluid and the turbine in the model.

To determine the diameter of the MRF an initial mesh was chosen and the diameter of the MRF was increased from a starting value of $1\,\mathrm{m}$ to see how the performance of the turbine was affected. The results from this can be seen in Table II. The initial mesh was largely unrefined in the outer control volume as the proximity of the MRF to the blades would be the main factor affecting the results. It was found that beyond a diameter greater than 1.3m the torque and thrust values were unchanged.

TABLE III: *Performance coefficients in relation to MRF diameter.*

MRF Diameter (m)	Torque (Nm)	C_P	Thrust (N)	C_T
1	18.32	0.432	266.5	0.84
1.1	18.47	0.435	266.5	0.84
1.3	18.49	0.436	266.6	0.84
1.7	18.49	0.436	266.6	0.84
2.1	18.49	0.436	266.6	0.84

A mesh independence study was conducted to initially give an idea of the expected performance of the turbine. The area of main interest was the face sizing on the blades and the mesh density in the MRF. The mesh was largely unstructured and used tetrahedral elements. To reduce the number of elements in the hope of keeping the computational time down the mesh sizing on the blade became gradually more refined towards the tip of the blade as it moved away from the root. The smallest element size on the blade was $0.003\,\mathrm{m}$ gradually increasing to $0.007\,\mathrm{m}$ at the blade root. To achieve this the blade was broken down into three faces, the tip, the middle and the root. Each of these three faces could then have a face sizing applied directly onto it allowing more control on the mesh size. The remainder of the MRF was given a sizing of $0.02\,\mathrm{m}$. The outer domain was limited to a maximum size of $0.2\,\mathrm{m}$.

The reason for the large sizing in the control volume was because the wake was of less interest within this work so was subsequently of secondary interest during the mesh independence study. By keeping a larger mesh sizing the total number of elements could be reduced thus reducing the computational complexity and solver time.

A domain interface was used to pass information between the two domains. The sizing of the mesh on the domain interface was also manually refined so that the same sizing was applied to both sides of the interface to reduce any solver issues. The final mesh contained around 3 million elements, with around 1.2 million of these being contained within the MRF.

CFX Pre was used to set up the boundary conditions for the problem. The inlet was given a flow velocity of $1\,\mathrm{m\,s^{-1}}$, the walls were set to a no slip condition to account for the frictional effect of the tow tank. The top was left as an opening and the outlet was given a static pressure of $0\,\mathrm{Pa}$ as the problem in question was not pressure driven. The turbine blades, hub and stanchion were all given the no slip wall condition.

To create the rotation desired a MRF was used as it allows a rotational component to be added to the model. The angular velocity could be set in accordance with the desired tip speed ratio (TSR). A range of TSR's between 0 and 7.5 were run within the model. Both steady state and transient models were initially looked at to determine the difference, if any, between the performance coefficients. It was found that the difference between the results was less than $2\,\%$ as seen in Table IVso the steady state model was used going forward to help reduce the computational time.

TABLE IV: *Steady state and transient results comparison.*

Model Type	C_P	C_T
Steady State	0.421	0.836
Transient	0.428	0.849
Percentage Difference	1.6	1.5

Within the steady state model the turbine itself is not moving, rather the water in the MRF is subject to the rotational velocity denoted in the setup. The result is not dependent on time and is a time-averaged value over the duration of the model. Transient models use a sliding mesh approach to simulate the rotation of the turbine with respect to time and the values for torque and thrust can be seen at each time step if required.

The SST k-omega turbulence model was used to close the RANS equations due to the improved performance in adverse pressure gradients when compared to the k-epsilon or k-omega models individually [19].

Experimental validation was required for the model and testing was conducted in the INSEAN tow tank facility. The outer control volume used the same cross sectional dimensions as the INSEAN tank. Details for this can be found in Section II-D.

D. Experimental

The experimental testing was conducted in the tow tank facility at INSEAN. The dimensions of the tank were $9\,\mathrm{m}$ (width) x $3.5\,\mathrm{m}$ (depth) x $220\,\mathrm{m}$ (length). The turbine was fixed to the carriage with the centre of the turbine being placed $1.5\,\mathrm{m}$ below the surface of the water. The blockage ratio for the tow tank was around $2\,\%$ so no correction factor was needed [20].

The turbine was operated under speed control according to the desired TSR. The acceleration and slowing of the carriage meant that the useful usable distance was reduced to around $190\,\mathrm{m}$. Between each run the turbine was brought back to that start position and then the tank left to settle so any turbulence generated from the previous run would dissipate. Two TSR cases were measured each run to maximise the time available for testing.

The set up for the turbine can be seen in Fig. 2. Despite the carriage velocity being set to the desired speed a pitot tube was also used to give a second measure for the tow speed. The tow speed of the carriage was $1\,\mathrm{m\,s^{-1}}$. A valeport current measuring device can also be seen however this was not used during the characterisation runs.

III. Results and Discussion

To identify the optimum blade design the BEMT results were looked at allowing the design of the 3D blade for use in the CFD model and for manufacture in the workshop. The experimental results were looked at and compared with the results obtained from testing of the old turbine to determine the changes in performance. Next the CFD and experimental results were compared with the aim of providing validation for the computational models. Lastly the two computational methods were compared to see how each faired at predicting the performance of a tidal turbine.

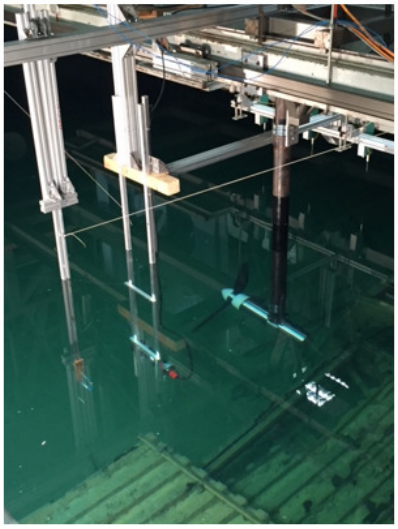

Fig. 2: *INSEAN tow tank set up.*

A. BEMT

When looking at the results from the BEMT models the range of chord lengths and blade twists mentioned in Section II-B were all compared. The optimum chord length distribution was found to be that of Blade 1 as seen in Table II. Out of the range of twist distributions mentioned in Section II-B the 4 with the highest performance coefficients were plotted against each other for comparison. The power coefficient for the 19 degree twist distribution was found to be the highest as shown in Fig. 4. The peak C_P was just over 0.45 at a TSR of 3.5.

Fig. 3: *Old blade (left) and the new blade (right)*

From this point onwards when talking about the blade, the chord lengths and twist are those of Blade 1 in Table II and 19 degrees respectively. A comparison between the new design and the old design can be seen in Fig. 3. It is worth noting that the attachment method of the blade to the hub due to the design on the turbine. The pin on the base of the old blade was previously used where as the new blade contains a bore hole in the base that a pin fits into and is grub screwed in place.

Fig. 5 shows the C_T for the same cases. It can actually be seen that the 19 degree case has the highest thrust coefficient over the entire range of TSR's when compared to those of 20 - 22. One of the initial criteria was to keep the C_T within 10 %. So despite the C_T being higher for the 19 degree case it was still within the remit of the design and so due this design having the highest value of C_P compared to the other models it was chosen going forward.

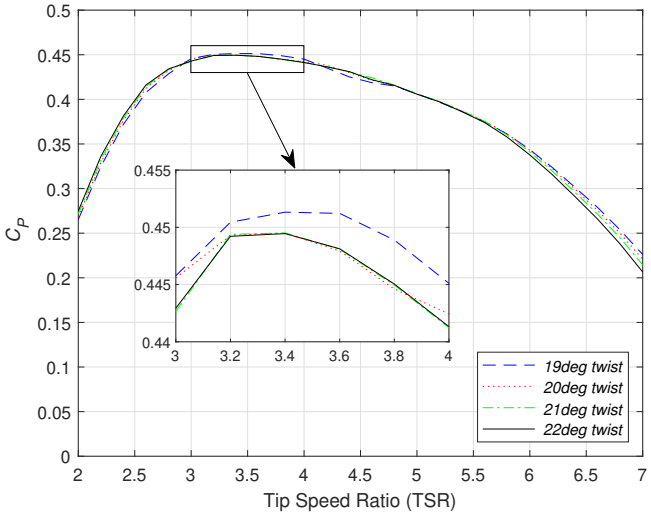

Fig. 4: *Comparison of the BEMT C_P predictions for twist distributions between 19-22 degrees*

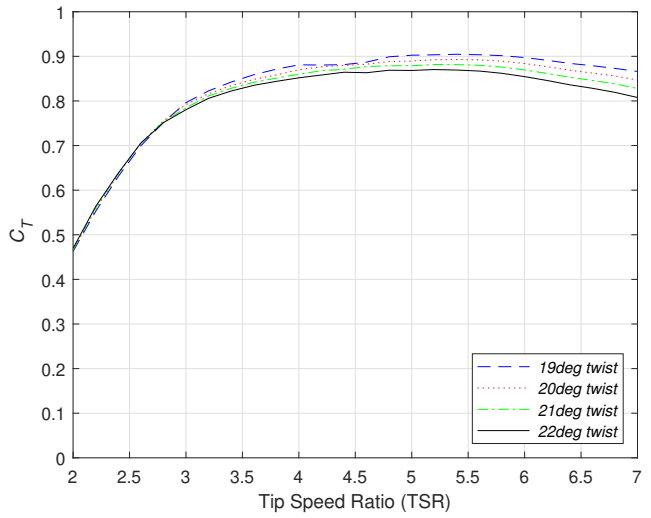

Fig. 5: *Comparison of the BEMT C_T predictions for twist distributions between 19-22 degrees*

The geometrical design of the blade was, at this point, complete and could be modelled for use in the CFD set up. The pitch angle for the old blade was 6 degrees and so to determine the optimised set up for the blade a range of pitch angles between 5 - 8 degrees were looked at. The power and thrust coefficients for these pitch angles can be seen in Fig. 6 and 7 respectively.

The pitch angle of 8 degrees was found to have the highest C_P at $\approx$ 0.45 while also having a low C_T of $\approx$ 0.88 at peak TSR. SolidWorks was used to produce the three dimensional drawing of the blade. The final blade was 384.5 mm from root to tip with a

twist of 19 degrees. The pitch angle was set to 8 degrees for all the corresponding CFD an experimental models.

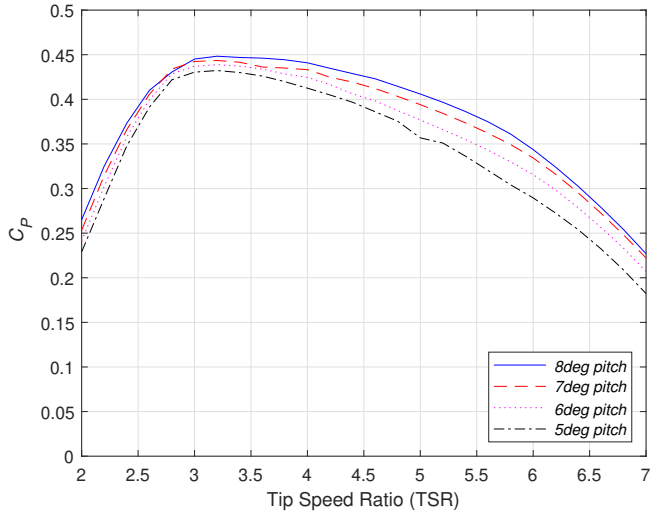

Fig. 6: *Comparison of the BEMT C_P predictions for pitch angles of 5-8 degrees*

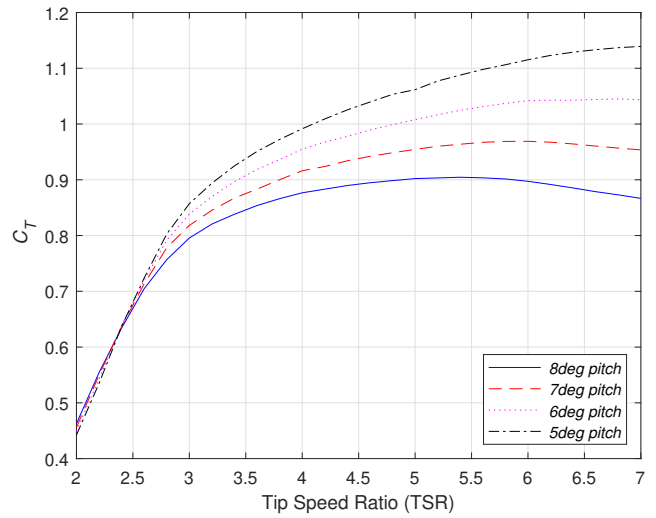

Fig. 7: *Comparison of the BEMT C_T predictions for pitch angles of 5-8 degrees.*

B. Experimental

The experimental work was carried out in the INSEAN tow tank facility as discussed in Section II-D. The results for power and thrust coefficients are shown in Fig. 8 and 9 respectively. Due to the time constraints when testing, TSR values above 1.5 and below 5.5 were not looked at. The aim of this was to try and get good characterisation of the turbine in the region of peak power. Peak power for the old turbine was approximately 3.65 and so again this area was looked at with more interest.

The error bars shown for both the C_P and C_T represent $+/-$ the standard deviation. This deviation is not a quote on the uncertainty of the measurements but rather the fluctuations seen in the recorded measurements from each run. During each run two values of TSR were recorded, again due to time constraints. The total time for recording the data was close to 180 s at a sample rate of 200 Hz. The time was split evenly between the two TSR values. A small period of time was allowed in-between to account for the change in the speed control so that the turbine could reach the necessary rotational velocity.

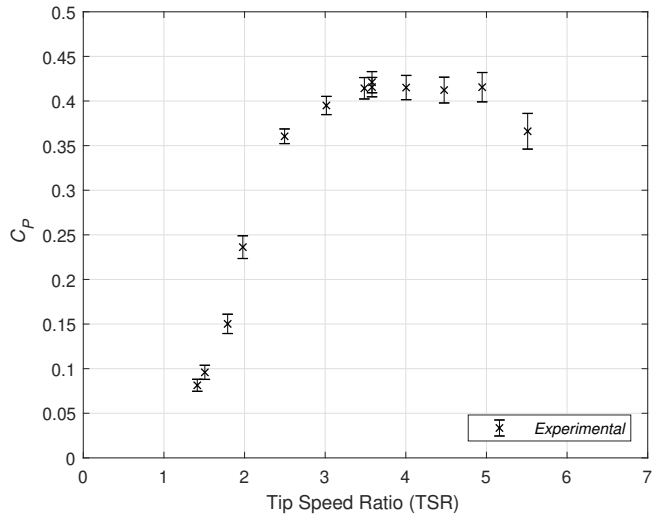

Fig. 8: *Experimental data with repeats for C_P*

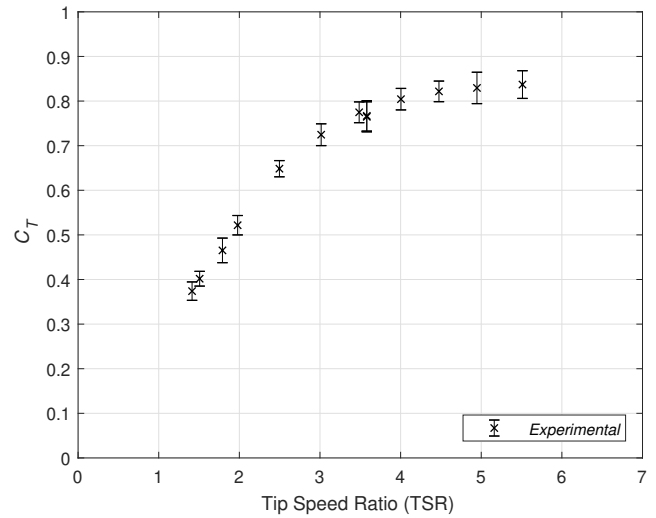

Fig. 9: *Experimental data with repeats for C_T*

Repeat runs were done for the region around peak C_P. As can be seen in both Fig. 8 and 9 the repeatability of the results is good. Very little difference, in the order of 2.5 %, is seen between 3 runs at a TSR of 3.6 falling comfortably within the standard deviation of the measurements.

One of the criteria when setting out was to ensure that the C_T was not greatly increased when compared to the original design. By looking at the experimental results the C_T was found to be around 0.81 at peak power. The second objective was to increase the C_P for the turbine. Fig. 10 shows a comparison between the new blade being tested at the INSEAN facility and the old blade being tested at the Liverpool Flume. One thing to mention about the experimental testing for the old turbine was that the Liverpool flume dimensions mean that the blockage ratio is 17.5 %. No correction factors have been added when calculating these results, which should be the case

according to Garrett and Cummins [21] otherwise what is seen is an artificially high value of C_P.

The power coefficients for the original turbine also drops away much quicker towards free-wheeling as it reaches higher TSR values. With regards to the new blade this effect is not quite as dramatic. The C_T plots have not been included for the old blade due to problems with the measurement systems during the testing campaign. From extensive modelling however by [22] the C_T was found to be in the region of 0.85.

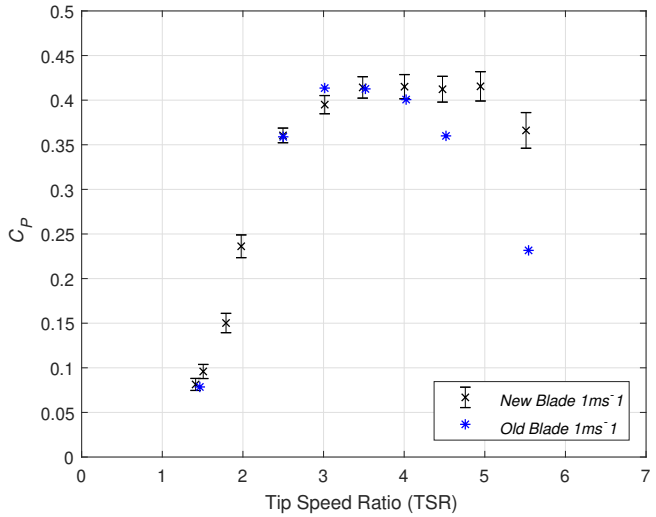

Fig. 10: *Experimental data comparison between the old and new blades at* $1\,\mathrm{m\,s^{-1}}$ *for* C_P

C. CFD Validation

The CFD model was set up to directly replicate the INSEAN tow tank geometry, however the length of the model did not need to be $190\,\mathrm{m}$ and was therefore reduced to $20\,\mathrm{m}$ to reduce the computational time, while also ensuring the outlet had no impact on the results. By looking at Fig. 11 it can be seen that the CFD models correspond very closely with the values from INSEAN for the C_P. The stanchion was included within the CFD model so as to keep everything as close as possible.

Similarly for the C_T values shown in Fig. 12 good agreement is seen between the CFD and experimental results up to peak TSR.

A slight discrepancy can be seen for TSR values greater than 5, however for reasons mentioned in Section III-B fewer readings were taken in the higher TSR region making it hard to comment on whether the two curves would collapse down onto each other.

The results show that the CFD model provides a good comparison to experimental testing as seen from the similarities in the results for both the performance characteristics.

D. Computational Comparison

Due to the similarity in the CFD model and experimental results as shown in Section III-C a comparison was then drawn between the two computational methods used during the work. The CFD model included the stanchion and the thrust was taken from the blades and the hub. However within BEMT the stanchion is not accounted for and only the thrust on the blades is calculated. A second CFD model, still using the INSEAN geometry, was set up however this time the stanchion was removed from the model and the thrust acting on the hub was not included when calculating the thrust coefficient.

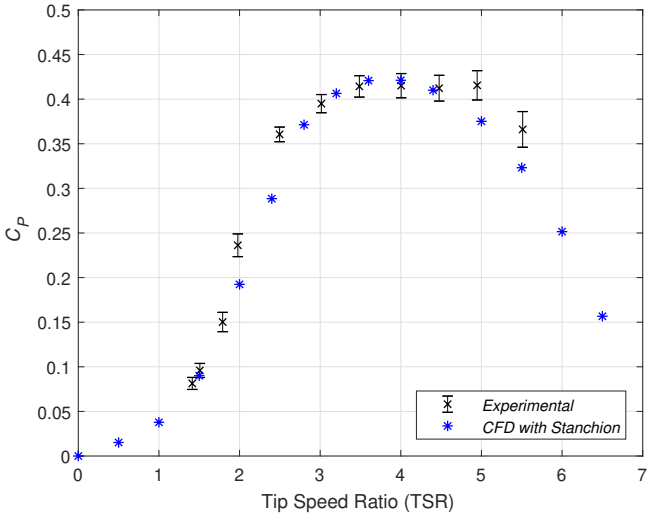

Fig. 11: *Comparison between experimental and CFD models with the inclusion of the stanchion for* C_P

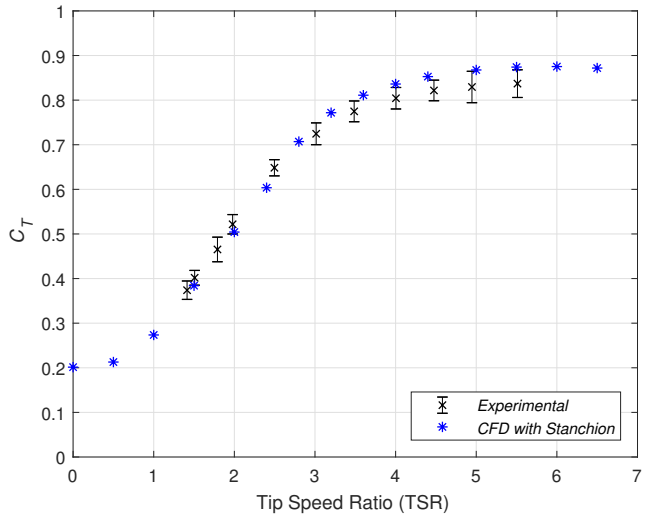

Fig. 12: *Comparison between experimental and CFD models with the inclusion of the stanchion for* C_T

The results from the three different models are shown in Fig. 13 and 14. The values for the BEMT in the lower TSR region, less than TSR 2, have been ignored. One reason for this is that because BEMT solves for a 2D aerofoil no 3D, or span wise, flow is accounted for and so stall delay can become an issue, leading to an inaccuracy in predicting the low TSR performance characteristics of a turbine [23], [24].

By comparing the BEMT to the CFD model that includes the stanchion it can be seen that the BEMT over predicts both the power and thrust coefficients. As mentioned earlier this could be down to the fact that the stanchion has not been taken into consideration as part of the BEMT calculation. The flow directly behind the blades will have a lower velocity due to the blockage of the stanchion on the fluid. The proximity of the blade to the stanchion can cause the area of lower flow velocity to attach to the back of the blade and ultimately reduce the performance of the blade passing the stanchion [22].

If the stanchion is then removed from the CFD model and

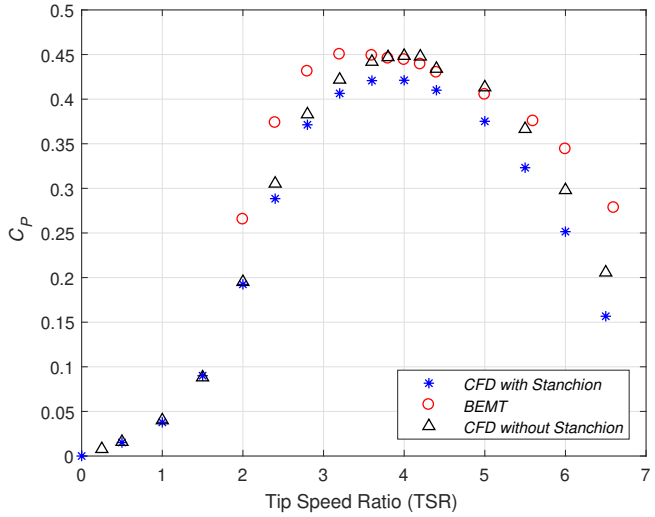

Fig. 13: *Comparison of the C_P between CFD and BEMT*

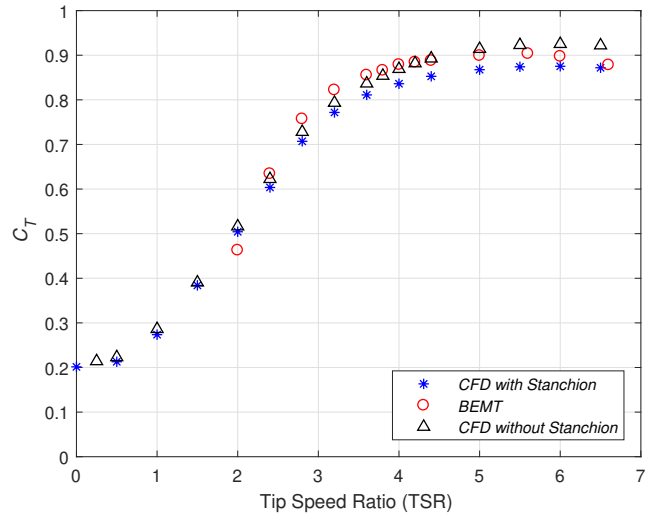

Fig. 14: *Comparison of the C_T between CFD and BEMT*

compared with the BEMT results then what we see is a much closer comparison between both the trust and the power coefficient as the blockage from the stanchion is no longer an issue within the model. BEMT still seems to over predict for both the of the coefficients, however around the peak of the curve the grouping is close. The disagreement comes at the higher and lower range of TSR values which fits with reasons mentioned earlier when comparing the BEMT results to the CFD model with the stanchion.

IV. Conclusion

When setting out the aim of the work was to look at a new blade design, based on the Wortmann FX63-137 aerofoil, that improved the C_P when compared to the old blade modelled at Cardiff University.

BEMT and CFD were used in order to produce a new design. The experimental model was set up to give validation to the numerical methods being used. The secondary aim was to see how BEMT and CFD performed, both against each other and against the experimental model, when predicting the performance of a tidal turbine for use in future work.

A visible improvement in the power coefficient of the turbine was seen when compared to the original blade design. BEMT was used as the initial method for designing the new blade and so from this it can be said that it is a useful tool when looking to change the design of a turbine blade. Despite its limitation it does offer a quick and accurate blade design procedure.

CFD was shown to have good agreement with the experimental results when modelled directly. Very little difference was seen between the results at the peak of the power curve. However when comparing BEMT to the CFD model with the stanchion it could be seen the BEMT over predicted for both the C_P and C_T. Despite BEMT giving a good indicator of blade performance, when it comes to simulating a deployed turbine it over predicts the performance characteristics.

The CFD model without the stanchion and the BEMT model also showed a good agreement except at the lower TSR regions, the reasons for which are discussed in Section III-D.

V. Acknowledgements

The authors acknowledge support from SuperGen UK Centre for Marine Energy (EPSRC: EP/N020782/1) and MaRINET II Transnational Access Program. The authors would also like to thank the staff members at INSEAN for their assistance during testing. This work was performed using the computational facilities of the Advanced Research Computing @ Cardiff (ARCCA) Division, Cardiff University. Authors are grateful to PRIMaRE for supporting the travel to this event through an Early Career Research Travel Grant (ECR-TG), which has received funding from EPSRC under grant agreement EP/P026109/1.

References

[1] DECC (Department of Energy and Climate Change). UK Renewable Energy Roadmap Update 2013. (November):76, 2013.

[2] The Carbon Trust. Accelerating Marine Energy. *The Carbon Trust*, (July):1–64, 2011.

[3] MeyGen. The MeyGen Project.

[4] DA Egarr, T O'doherty, S Morris, and RG Ayre. Feasibility study using computational fluid dynamics for the use of a turbine for extracting energy from the tide. ... *Fluid Mechanics* ..., (December):1–4, 2004.

[5] Michael S. Selig and Bryan D. McGranahan. Wind Tunnel Aerodynamic Tests of Six Airfoils for Use on Small Wind Turbines. *Journal of Solar Energy Engineering*, 126(November):986, 2004.

[6] Ju Hyun Lee, Sunho Park, Dong Hwan Kim, Shin Hyung Rhee, and Moon Chan Kim. Computational methods for performance analysis of horizontal axis tidal stream turbines. *Applied Energy*, 98:512–523, 2012.

[7] P. B. Johnson, G. I. Gretton, and T. McCombes. Numerical modelling of cross-flow turbines: a direct comparison of four prediction techniques. *3rd International Conference on Ocean Energy*, pages 2–6, 2010.

[8] Ian Masters, Alison Williams, T. Nick Croft, Michael Togneri, Matt Edmunds, Enayatollah Zangiabadi, Iain Fairley, and Harshinie Karunarathna. A comparison of numerical modelling techniques for tidal stream turbine analysis. *Energies*, 8(8):7833–7853, 2015.

[9] T O 'Doherty, A Mason-Jones, D M O 'Doherty, C B Byrne, I Owen, and Y X Wang. Experimental and Computational Analysis of a Model Horizontal Axis Tidal Turbine. *8th European wave and tidal energy conference*, (m):833–841, 2009.

[10] A. Mason-Jones. Performance assessment of a horizontal axis tidal turbine in a high velocity shear environment. 2010.

[11] Mark Drela. XFOIL: An Analysis and Design System for Low Reynolds Number Airfoils. *Lecture Notes in Engineering*, 54(October):1–12, 1989.

[12] A. F. Molland, A. S. Bahaj, J. R. Chaplin, and W. M. J. Batten. Measurements and predictions of forces, pressures and cavitation on 2-D sections suitable for marine current turbines. *Proceedings of the Institution of Mechanical Engineers, Part M: Journal of Engineering for the Maritime Environment*, 218(2):127–138, 2004.

[13] Chul-hee Jo and Kang-hee Lee. Application of an Airfoil to the Tidal Turbine Design by Analyzing Two-dimensional Performance in the Water. (Eesd):123–138, 2017.

[14] J. Morgado, R. Vizinho, M. A.R. Silvestre, and J. C. Páscoa. XFOIL vs CFD performance predictions for high lift low Reynolds number airfoils. *Aerospace Science and Technology*, 52:207–214, 2016.

[15] I Masters, J C Chapman, M R Willis, and J A C Orme. A robust blade element momentum theory model for tidal stream turbines including tip and hub loss corrections. 4177(June), 2016.
[16] H Glauert. *The elements of aerofoil and airscrew theory*. Cambridge University Press, 1946.
[17] Martin O.L Hansen. *Aerodynamics of Wind Turbines*. 2015.
[18] T. M. Nevalainen, C. M. Johnstone, and A. D. Grant. A sensitivity analysis on tidal stream turbine loads caused by operational, geometric design and inflow parameters. *International Journal of Marine Energy*, 16:51–64, 2016.
[19] F R Menter. A comparison of some recent eddy-viscosity turbulence models. *Journal of Fluids Engineering, Transactions of the ASME*, 118(3):514–519, 1996.
[20] Robert Howell, Ning Qin, Jonathan Edwards, and Naveed Durrani. Wind tunnel and numerical study of a small vertical axis wind turbine. *Renewable Energy*, 35(2):412–422, 2010.
[21] Chris Garrett and Patrick Cummins. The efficiency of a turbine in a tidal channel. *Journal of Fluid Mechanics*, 588:243–251, 2007.
[22] Carwyn Frost. *Flow Direction Effects On Tidal Stream Turbines*. PhD thesis, 2016.
[23] J. L. Tangler. Comparison of Wind Turbine Performance Prediction and Measurement. *Journal of Solar Energy Engineering*, 104(2):84–88, 1982.
[24] Andreas Gross, Hermann Fasel, Tillmann Friederich, and Markus Kloker. Numerical Investigation of S822 Wind Turbine Airfoil. *40th Fluid Dynamics Conference and Exhibit*, (November):1–25, 2010.